JMEPEG (2010) 19:1104–1115
DOI: 10.1007/s11665-009-9592-6

1059-9495/$19.00

Spatial Modulation and Filtering of Diffusion Patterns for Inverse Analysis of Heat Deposition

S.G. Lambrakos

(Submitted November 18, 2009)

General parameterizations are constructed for spatial modulation and filtering of heat diffusion patterns according to general energy deposition characteristics occurring within a volume of material resulting from a volumetrically coupled energy source. These parameterizations include previously constructed models of energy deposition as special cases. The construction of a general parameterization of energy deposition processes is necessary for their inverse analysis. The structure of such a parameterization follows from the concepts of model and data spaces that imply the existence of an optimal parametric representation for a given class of inverse problems. Accordingly, the optimal parametric representation is determined by the characteristics of the available data, which in principle can contain both experimental measurements and numerical simulation data. Parameterizations for spatial modulation and filtering of heat diffusion follow from the observation that many different types of energy deposition processes can be represented by weighted sums of basis functions whose general forms are that of spatially modulated or filtered diffusion. A significant aspect of the parameterizations presented is that the definition of the inverse heat deposition problem, which is adopted for their construction, provides a rigorous foundation for a highly flexible and general parameterization of energy deposition processes, which is essential for their inverse analysis. A preliminary proof is presented that shows the significance of these parameterizations for the application of similarity transformations to the inverse analysis of energy deposition processes. The applicability of similarity transforms to the inverse analysis of heat deposition is another property that follows from the specific definition of the inverse heat deposition problem considered here.

Keywords joining, modeling processes, welding

1. Introduction

The inverse problem approach is optimal for system characterization in that it tends to adopt large amounts of available data for model input (Ref 1-9). Considered here is a particular class of inverse analysis methods that are applied to heat deposition processes where the available data consists of temperature distributions, or information related to these distributions, over and within bounded spatial domains. Or equivalently, the available data consists of temperatures distributed over essentially closed surfaces spanning regions of finite volume containing materials of interest. The determination of the temperature field within a bounded domain defines an inverse heat deposition problem, which represents a particular category of the more general inverse problem concerning inverse analysis of heat transfer (Ref 10-18). Other investigators have also focused on various aspects of inverse problems related to heat deposition processes especially as they relate to the determination of heat fluxes via appropriate regularization of their spatial and time distributions (Ref 19).

S.G. Lambrakos, Materials Science and Technology Division, Code 6390, Naval Research Laboratory, Washington, DC 20375-5320. Contact e-mail: lambrakos@nrl.navy.mil.

General aspects of the inverse-problem approach presented here, for the analysis of heat deposition processes, have been studied (Ref 20-30). These studies considered the specific physical characteristics of heat deposition processes that are relevant to using this inverse-problem approach for their analysis. This approach included the use of effective material properties and heat source distributions as adjustable quantities. These quantities are adjusted according to experimental data in order to constrain the temperature field self-consistently. Throughout these studies prototype analyses were presented in order to demonstrate many of the details associated with practical application of this inverse-problem approach and its use for extraction of process parameters and parameters that may be correlated with material properties. The general parameterization of heat deposition systems follows from the concept of a model space that establishes the existence of an optimal parametric representation for a given class of inverse problems. This property is related to the fact that inverse analyses based entirely on mathematical formulations representing physical theories are not generally well posed in that these formulations are inherently based on direct-problem paradigms. The term "well posed" here for an inverse problem is used in the sense of Hadamard (Ref 31), which is such that a problem is well posed if a solution exists, this solution is unique and it depends continuously on the data. In particular, the concept of a model space implies the existence of an optimal parametric representation for inverse analysis, which is not based on the existence of a complete set of representative physical theories, but rather on the characteristics, relative sizes and completeness of data sets associated with or in practice available for that system, i.e., the data space. Some collected works, within which there are comprehensive reviews of models of energy deposition processes and their associated parameterizations, are the "Trends in Welding" series (see Ref 32), the "Mathematical Modelling of Weld Phenomena" series (see Ref 33), and the works of Goldak et al. (Ref 34-36). The parameterizations presented in this study are constructed according to the following concepts, some of which have been discussed previously.

1.1 Generalized Functions

A generalized function is defined as a function representation of a class of functions, rather than a specific function, where the class of functions is characterized by a specific set of trend features (Ref 37). This concept was introduced in signal processing, where for many analysis applications specific trend features are of significance rather than specific analytical forms. In what follows the concept of generalized functions is extended for the construction of general basis functions for parametric representation of energy deposition processes.

1.2 Parameterization Using Basis Functions

The inverse analysis approach considered here adopts a model space where each point of this space represents a set of basis functions, in contrast to any "conceivable" model, for parametric representation in terms of weighted sums of these functions. The specific set of basis functions are to be selected according to two criteria. These are their relative optimality for establishing a mapping from data space to system output and for the inclusion of information concerning physical characteristics of the system, i.e., a gray box parametric representation.

1.3 General Characteristics of Energy Deposition

The inverse analysis approach considered here assumes a general partitioning of energy deposition processes into two separate spatial domains. One domain is that containing the volumetric distribution of energy within the material of the workpiece due to coupling with the energy source. The other domain is that containing the temperature field distribution within the workpiece. The nature of the coupling between these two domains is assumed phenomenological in that the characteristic time and spatial scales for the physical processes in each of the domains is significantly different from that of the other. An advantage of the inverse analysis approach is that an explicit consideration of the nature of the coupling between these domains is not necessary. An important aspect of the temperature field distribution associated with energy deposition processes is the presence of two types of weighting. These are weighting due to the presence of a surface boundary that is at the origin of coupling of energy into the system; and weighting due to the relative motion of the energy source and workpiece. The presence of these weightings provides for filter properties that tend to make the temperature field distribution insensitive to small-scale temporal and spatial features of the volumetric distribution of energy.

1.4 Volumetric Source Function

The volumetric energy source function, or equivalently, parametric representation of the volumetric distribution of energy within the material of the workpiece, is the primary component for mathematical representation of energy deposition processes for both direct and inverse analyses. Accordingly, many researchers have constructed different types of source functions for different types of energy deposition processes (Ref 34-58). A review of the different source function formulations from the perspective of inverse analysis, however, shows that these functions are within a specific class of functions. Therefore, it follows that one can construct a "generalized function" representation of the volumetric distribution of energy that includes previously constructed source functions as special cases.

1.5 Parameterizations for Modulation and Filtering

Parameterizations for diffusion pattern modulation follow from the observation that many different types of energy deposition processes can be represented by weighted sums of basis functions whose general forms are that of spatially modulated diffusion. Similarly, parameterizations for diffusion pattern filtering follow from the observation that many specific features of energy deposition processes can be characterized by directionally or path weighted diffusion. A significant aspect of the parameterizations presented here is that the statement of the inverse heat deposition problem adopted for their construction provides a rigorous foundation for a general parameterization of energy deposition processes, which includes modulation and filtering of diffusion patterns.

The organization of the subject areas presented here is as follows. First, a precise mathematical statement of the inverse problem to which the analysis methodology is to be applied is given. In that the range of inverse problems is vast, it is essential, even within the context of inverse heat transfer, to define precisely the inverse problem to be addressed. Second, parameterizations are constructed for spatial modulation and filtering of heat diffusion patterns that use weighted sums of analytical basis functions. Third, a discussion is given concerning the construction of temperature-field parameterizations using numerical basis functions. Fourth, a prototype analysis is presented for the purpose demonstrating various aspects of parameterizations that represent spatial modulation and filtering. This section also includes calculations demonstrating various aspects of spatially modulated and filtered heat diffusion patterns according to the general physical characteristics of energy deposition within a volume of material resulting from a volumetrically coupled energy source. Fifth, a preliminary proof is presented that shows the significance of these parameterizations for the application of similarity transformations to the inverse analysis of energy deposition processes. And finally, a concluding discussion is presented.

2. Definition of Inverse Heat Deposition Problem

The inverse problem concerning analysis of physical processes, in general (Ref 1-9), and the inverse heat transfer problem, in particular (Ref 10-18), may be stated formally in terms of source functions (or input quantities) and multidimensional fields (output quantities). The statement of the inverse problem given here is focused on aspects of inverse heat deposition problem related to the determination of heat fluxes via appropriate regularization of their spatial and time distributions. This statement represents an extension of that given in Ref 19. In general, the formulation of a heat conductive system occupying an open bounded domain Ω with an outer boundary

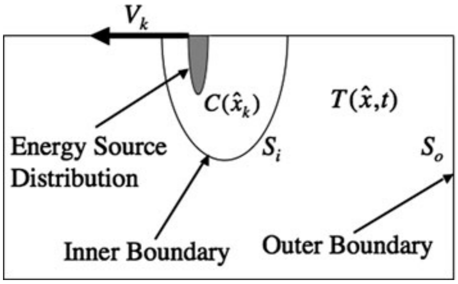

Fig. 1 Schematic representation of inner and outer boundaries of temperature field that define inverse heat deposition problem, and weighting influences on temperature field associated with energy deposition

S_o and an inner boundary S_i (see Fig. 1) involves the parabolic equation

$$\frac{\partial T(\hat{x},t)}{\partial t} = \nabla \cdot (\kappa(\hat{x},t)\nabla T(\hat{x},t)) \qquad \text{(Eq 1a)}$$

for $T(\hat{x},t)$ in $\Omega \times (0,t_f)$, with initial condition $T(\hat{x},0) = T_0(\hat{x})$ in Ω, and heat flux exchanges through the outer and inner boundaries S_o and S_i as follows:

$$-\kappa(\hat{x},t)\frac{\partial T(\hat{x},t)}{\partial n_{S_o}} = c(\hat{x},t)(T(\hat{x},t) - T_a(\hat{x},t)) \qquad \text{(Eq 1b)}$$

on $S_o \times (0,t_f)$, and

$$-\kappa(\hat{x},t)\frac{\partial T(\hat{x},t)}{\partial n_{S_i}} = q(\hat{x},t) \qquad \text{(Eq 1c)}$$

on $S_o \times (0,t_f)$. Here $\hat{x} = (x,y,z)$ is the position vector, $n_{S_o}$and n_{S_i} are the normal vectors onto boundary S_o and S_i, respectively, t is the time variable, t_f is the final time, $T(\hat{x},t)$ is the temperature field variable, $\kappa(\hat{x},t)$ is the thermal diffusivity field variable, $c(\hat{x},t)$ and $T_a(\hat{x},t)$ are specified functions, and $q(\hat{x},t)$ is the heat flux on the inner boundary S_i. Determination of the temperature field via solution of Eq 1a-1c defines the direct initial-boundary value problem. The inverse problem considered here is that of effectively reconstructing the heat flux field $q(\hat{x},t)$ on the inner and outer boundaries S_i, and the resulting temperature field $T(\hat{x},t)$ for all time $t \in [0,t_f]$ when S_i and S_o are totally or partially inaccessible. In order to reconstruct the heat flux, information on the temperatures $T(\hat{x}_s,t)$, where $\{\hat{x}_s\} \in S_i, S_o$ is needed and therefore must be acquired either experimentally or via direct numerical simulation (Ref 20-30).

Following the gray-box inverse analysis approach, a parametric representation based on a physical model provides a means for the inclusion of information concerning the physical characteristics of a given energy deposition process. It follows then that for heat deposition processes involving the deposition of heat within a bounded region of finite volume, consistent parametric representations of the temperature field are given by

$$T(\hat{x},t,\kappa) = T_A + \sum_{k=1}^{N_k} T_k(\hat{x},\hat{x}_k,t,\kappa;\alpha_1,\ldots,\alpha_n) \quad \text{and}$$
$$T(\hat{x}_n^c,t_n^c,\kappa) = T_n^c \qquad \text{(Eq 2)}$$

where the quantity T_A is the ambient temperature of the workpiece and the locations $\hat{x}_n^c$ and temperature values T_n^c specify constraint conditions on the temperature field. The functions $T_k(\hat{x},\hat{x}_k,t,\kappa;\alpha_1,\ldots,\alpha_n)$ represent an optimal basis set of functions for given sets of boundary conditions and material properties. The quantities $\hat{x}_k = (x_k,y_k,z_k)$, $k = 1,\ldots, N_k$, are the locations of the elemental source or boundary elements. The sum defined by Eq 2 can for certain systems specify numerical integration over the discrete elements of a distribution of sources or boundary elements. Selection of an optimal set of basis functions is based on a consideration of the characteristic model and data spaces of heat deposition processes and subsequently isolating those regions of the model space corresponding to parameterizations that are both physically consistent and sufficiently general in terms of their mathematical representation and mapping from data to model space. Although heat deposition processes may be characterized by complex coupling between the heat source and workpiece, as well as complex geometries associated with either the workpiece or deposition process, in terms of inverse analysis the general functional forms of the temperature fields associated with all such processes are within a restricted class of functions, i.e., optimal sets of functions. Accordingly, a sufficiently optimal set of functions are the analytic solutions to heat conduction equation for a finite set of boundary conditions (Ref 59). A parameterization based on this set is both sufficiently general and convenient relative to optimization.

The formal procedure underlying the inverse method considered here entails the adjustment of the temperature field defined over the entire spatial region of the sample volume at a given time t. This approach defines an optimization procedure where the temperature field spanning the spatial region of the sample volume is adopted as the quantity to be optimized. The constraint conditions are imposed on the temperature field spanning the bounded spatial domain of the workpiece by minimization of the value of the objective functions defined by

$$Z_T = \sum_{n=1}^{N} w_n\left(T(\hat{x}_n^c,t_n^c,\kappa) - T_n^c\right)^2 \qquad \text{(Eq 3)}$$

where T_n^c is the target temperature for position $\hat{x}_n^c = (x_n^c,y_n^c,z_n^c)$.

The input of information into the inverse model defined by Eq 1a to 3, i.e., the mapping from data to model space is effected by the assignment of individual constraint values to the quantities T_n^c; the form of the basis functions adopted for parametric representation; and specifying the shapes of the inner and outer boundaries, S_i and S_o, respectively, which bound the temperature field within a specified region of the workpiece. The constraint conditions and basis functions, i.e., $T(\hat{x}_n^c,t_n^c,\kappa) = T_n^c$ and $T_k(\hat{x},\hat{x}_k,\kappa,t;\alpha_1,\ldots,\alpha_n)$, respectively, provide for the inclusion of the following types of information: (a) solidification cross-sections (e.g., transverse, longitudinal and top surface cross-sections); (b) spatial character of energy source (e.g., position of maximum temperature, shape and relative location of keyhole in deep-penetration welds); (c) geometric information (e.g., shape features of workpiece and top surface of weld); (d) boundary conditions on workpiece; (e) information related to temperature history (e.g., microstructure correlation with temperature); (f) thermocouple measurements; (g) energy input (e.g., energy per distance); and (h) information based on physical model representations of aspects of heat deposition process.

In a previous study (Ref 20), a partial proof was constructed for the existence of a general parametric representation for inverse analysis of heat deposition processes. This proof was considered partial in the sense that certain aspects of its development should be made more precise and investigated in more detail with respect to practical application. The essential components of this proof are as follows. First, the general trend features of heat deposition processes are such that the construction of a complete basis set of functions $T_k(\hat{x}, \hat{x}_k, t, \kappa; \alpha_1, \ldots, \alpha_n)$ making up a linear combination of the form defined by Eq 2 for representation of the associated temperature field is well defined and readily achievable. Second, for heat deposition processes, characteristics of the temperature field are poorly correlated to characteristics of the energy source. The characteristics of the temperature field that are associated with these processes, however, are strongly coupled only to inner boundaries on this field, e.g., the solidification boundary. This property follows from the low-pass spatial filtering property of the basis functions $T_k(\hat{x}, \hat{x}_k, t, \kappa; \alpha_1, \ldots, \alpha_n)$, whose general forms are consistent with the dominant trend features of heat deposition processes. Third, given a consistent set of basis functions, the temperature field associated with a heat deposition process is completely specified by the shape and temperature distribution of a given inner boundary on the domain of the temperature field; the diffusivity κ and speed of deposition V; and the lengths of the spatial dimensions D_i of the workpiece. Fourth, the shape and temperature distribution of a specified inner boundary S_i is determined by the rate of energy deposited on the surface of the workpiece and the strength of coupling of the energy source to the workpiece. And finally, in that an inner boundary S_i (see Fig. 1) is defined by its shape and the distribution of temperatures on its surface $T(\hat{x}_S)$, it follows that one can define a multidimensional temperature field $T(\hat{x}, \kappa, V, D, T(\hat{x}_S), \hat{x}_S \in S_{\mathrm{i}})$.

The existence of a convenient and general parameterization of inner boundary surfaces, $T(\hat{x}_S), \hat{x}_S \in S_{\mathrm{i}}$, bounding the temperature fields associated with heat deposition processes is conjectured based on the obvious fact that all heat deposition processes are characterized by thermal and energy deposition profiles whose general form can be represented by a small class of geometric shapes. This conjecture is plausible and is based on the fact that the observed volumetric distributions of energy from all types of heat deposition processes, within the inner boundary S_i of their associated temperature fields, can be represented by linear combinations of the basis functions that are within the class of generalized functions that are defined by the dominant trend features associated with volumetric energy deposition. These generalized functions provide for the construction of a relatively optimal and general parametric representation $T(\hat{x}, \kappa, V, D, T_S(\hat{x}_S), \hat{x}_S \in S_{\mathrm{i}}, S_{\mathrm{o}})$ for inverse analysis of heat deposition processes. In doing so, referring to Fig. 1, the inverse problem defined by the mapping

$$C(\hat{x}_k) \mapsto T(\hat{x}) \tag{Eq 4}$$

is replaced by the inverse problem defined by the mapping

$$C(\hat{x}_k), \kappa \mapsto S_{\mathrm{i}}, S_{\mathrm{o}} \mapsto T(\hat{x}). \tag{Eq 5}$$

Following the same arguments, the definition of the inverse heat deposition problem as given above can be extended to include systems that are characterized by incomplete information concerning the diffusivity function κ. This would include any nonlinear dependence of κ on temperature. This follows in that Eq 5 implies the existence of a weighted space averaged diffusivity.

Given an inverse analysis formulation that is defined by the sequence of mappings Eq 5, relatively interesting sensitivity issues are observed to follow. The mathematical properties underlying these sensitivity issues are the same as those responsible for the ill posedness of many inverse analysis procedures based on the mapping Eq 4. That is, those filter properties of diffusion processes that tend to make the temperature field $T(\hat{x})$ insensitive to details of the shape of the source distribution $C(\hat{x}_k)$ tend to make $T(\hat{x})$ insensitive to details of the shapes of S_{i} and S_{o}. This insensitivity to details of the shapes of S_{i} and S_{o}, e.g., the shape of the solidification boundary, implies that a general parametric representation of the inner and outer boundaries can in principle be formulated in terms of a reasonably convenient mathematical form. Presented in next sections are sensitivity analyses examining the sensitivity of $T(\hat{x})$ to shape features of S_{i} and S_{o} and relevance for inverse heat deposition analysis based on the sequence of mappings Eq 5. For these analyses the heat source distribution assumes the role of a boundary surface generator. This interpretation of $C(\hat{x}_k)$, which permits its convenient parameterization, provides a framework for parametrization of S_{i} and S_{o}.

In that the mapping $C(\hat{x}_k) \mapsto S_{\mathrm{i}}$ does not imply a unique energy source function $C(\hat{x}_k)$, the goal is to determine a relatively optimal basis function set for the generation of the inner surface boundary S_{i}. A general parameterization of the volumetric source function $C(\hat{x}_k)$ is constructed based on the general physical characteristics of energy deposition within a volume of material. This source function has been extended to represent secondary processes that are associated with deposition and includes previously constructed source functions as special cases. Accordingly, and following Galdak et al. (Ref 34-36) for representation of the influence of weighting due to motion of the energy source relative to the workpiece, for motion of the energy source along the x coordinate,

$$\begin{aligned} C(\hat{x}) = {} & \left([1 - u(x)] \cdot \exp\left[-a_1 x^2\right] + u(x) \cdot \exp\left[-a_2 x^2\right]\right) \\ & \times \exp\left[-by^2\right] \cdot Q(z), \end{aligned} \tag{Eq 6}$$

where $u(x)$ is the unit step function. The functional dependence of the volumetric source function with respect to depth of penetration is represented by the generalized function Q_g shown in Fig. 2, which is defined by three dominant trend features that are associated with primary and secondary processes, and their extinction. By adopting the generalized function Q_g, more convenient parameterizations can be employed according to the specific algorithm applied for

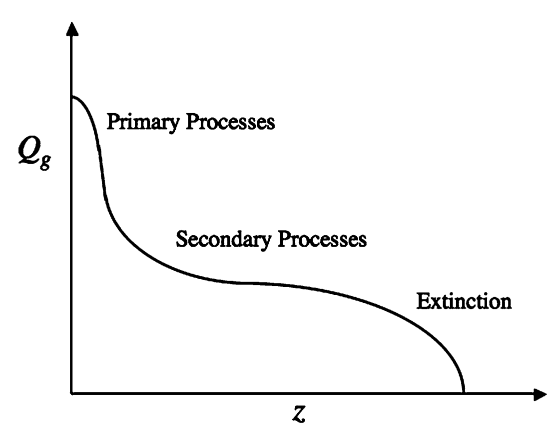

Fig. 2 Generalized function representation of volumetric energy distribution as a function of penetration depth that is characteristic of energy deposition processes

inverse analysis. A generalized function representation provides for the specification of numerical basis function representations of the source function. A discrete representation that should be convenient for numerical procedures applied to inverse analysis is defined by

$$Q(z) = \sum_{k=1}^{N_k} q(z_k)\delta(z - z_k), \tag{Eq 7}$$

such that $Q(z) \in Q_g, \delta(z)$ is the Dirac delta function, and $\{q(z_k), z_k\}$, $k = 1,\ldots,N_k$, represent adjustable parameters.

3. Parameterizations Using Analytical Basis Functions

In that energy deposition processes can in general be characterized by separate spatial domains corresponding to volumetric energy deposition and the resulting temperature field distribution, where the nature of the coupling between these two domains is a characteristic of the specific process, it follows that a consistent representation of the temperature field in terms of basis functions is of the form

$$T(\hat{x},t) = T_{\mathrm{A}} + \sum_{k=1}^{N_k}\sum_{n=1}^{N_t} C(\hat{x}_k)F(\hat{x},\hat{x}_k,n\Delta t,\kappa)\delta(n\Delta t - t_k), \tag{Eq 8}$$

where

$$F(\hat{x},\hat{x}_k,t,\kappa) = \frac{1}{t}\exp\left[-\frac{(x-x_k)^2 + (y-y_k)^2}{4\kappa t}\right] \times \left\{1 + 2\sum_{m=1}^{\infty}\exp\left[-\frac{\kappa m^2\pi^2 t}{l^2}\right]\cos\left[\frac{m\pi z}{l}\right]\cos\left[\frac{m\pi z_k}{l}\right]\right\}, \tag{Eq 9}$$

$t = N_t\Delta t$ and $\delta(t)$ is the Dirac delta function representing the instantaneous deposition at locations $\hat{x}_k = (x_k, y_k, z_k)$ at times $t = t_k$. The discrete speed of energy deposition V_k, which is an implicit function of position on the surface of the workpiece, is given by

$$V_k = \frac{x_k - x_{k-1}}{t_k - t_{k-1}}. \tag{Eq 10}$$

Accordingly, the procedure for inverse analysis defined by Eq 8-10 above entails adjustment of the parameters $C(\hat{x}_k)$, $\hat{x}_k$ and t_k defined over the entire spatial region of the workpiece. Another consistent representation of the temperature field in terms of basis functions is

$$T(\hat{x},t) = T_{\mathrm{A}} + \sum_{k=1}^{N_k}\sum_{n=1}^{N_t} C(\hat{x}_k)G(\hat{x} - V_k n\Delta t,\hat{x}_k,\kappa) \tag{Eq 11}$$

where

$$G(\hat{x},\hat{x}_k,t,\kappa) = \frac{1}{t}\exp\left[-\frac{(x-x_k-V_k t)^2 + (y-y_k)^2}{4\kappa t}\right] \times \left\{1 + 2\sum_{m=1}^{\infty}\exp\left[-\frac{\kappa m^2\pi^2 t}{l^2}\right]\cos\left[\frac{m\pi z}{l}\right]\cos\left[\frac{m\pi z_k}{l}\right]\right\} \tag{Eq 12}$$

Accordingly, the procedure for inverse analysis defined by Eq 11 and 12 above entails adjustment of the parameters

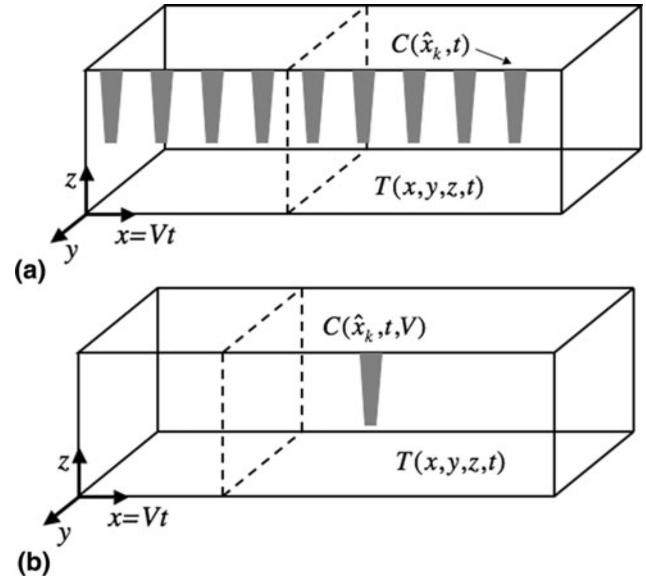

Fig. 3 Schematic representations of discrete source distributions corresponding to parameterizations defined by Eq 8-10 and Eq 11-12, respectively

$C(\hat{x}_k)$, $\hat{x}_k$, Δt and V_k defined over the entire spatial region of the workpiece. Shown in Fig. 3 are schematic representations of the discrete source distributions corresponding to the parameterizations defined by Eq 8 through 12.

At this stage it is necessary to establish an appropriate interpretation of the parameterizations expressed by the basis functions defined by Eq 8 through 12. First, it must be emphasized that the primary set of parameters for system representation, which are uniquely defined, are the quantities $(V, D, \kappa, T_s(\hat{x}_S), \hat{x}_S \in S_{\mathrm{i}}, S_{\mathrm{o}})$. And second, the weighted sums of basis functions defined by Eq 8 through 12 establish a set of parameters, which are not uniquely defined, such that

$$T(\hat{x}, t, V, D, \kappa, T_s(\hat{x}_S), \hat{x}_S \in S_{\mathrm{i}}, S_{\mathrm{o}}) = T(\hat{x}, t, \kappa, C(\hat{x}_k), \hat{x}_k, t_k, \Delta t, N_t, N_k, V_k). \tag{Eq 13}$$

Accordingly, the mapping from one set of parameters to another, defined by Eq 13, provides foundation for a general framework for spatial modulation and filtering of heat diffusion patterns for convenient construction of the temperature field $T(\hat{x}, t, V, D, \kappa, T_s(\hat{x}_S), \hat{x}_S \in S_{\mathrm{i}}, S_{\mathrm{o}})$.

4. Parameterizations Using Numerical Basis Functions

The set of basis functions presented above provide a general parametric representation for inverse analysis of heat deposition processes. Given these basis functions, the temperature field associated with any given heat deposition process is completely specified by a given set of inner and outer bounding surfaces S_{i} and S_{o}, respectively, the temperature distributions over these surfaces, the diffusivity κ, speed of deposition V, and the lengths of the spatial dimension D of the workpiece. Accordingly, it follows that one is able to define a multidimensional temperature field $T(\hat{x}, t, \kappa, V, D, T_s(\hat{x}_S), \hat{x}_S \in S_{\mathrm{i}}, S_{\mathrm{o}})$. It is significant to note, however, that this multidimensional field provides a parametric representation, i.e., parameterization, of heat deposition processes to the extent that any of the different possible types of boundary surfaces S_i and S_o, associated with these processes can be represented conveniently. This is certainly the case since the volumetric source function $C(\hat{x}_k)$ assumes the role of a boundary surface generator, and therefore provides a framework for parameterization of S_i and S_o using the basis functions given above.

A general procedure for construction of a multidimensional temperature field $T(\hat{x}, t, \kappa, V, D, T_s(\hat{x}_S), \hat{x}_S \in S_i, S_o)$ can now be described using the illustrative example that follows. The basis of this procedure is that for heat deposition processes, e.g., welding processes, associated with a given class of materials, e.g., metals, the range of different possible shapes of inner boundary surfaces S_i is denumerably finite and that diffusivities and workpiece dimensions are bounded within a relatively small range of values. Accordingly, a general procedure for construction of $T(\hat{x}, t, \kappa, V, D, T_s(\hat{x}_S), \hat{x}_S \in S_i, S_o)$, which is evolutionary, is based on the systematic accumulation of results of inverse analyses applied to various types of experimental measurements and numerical simulations. That is, the results of various inverse analyses, e.g., Ref 20-30, which involve different types of deposition processes can be stored. In addition, as in the illustrative example that follows, for a given inverse analysis where S_i has been specified, one can vary κ and D over their entire range of possible values and then store the associated temperature fields. A natural consequence of the finite range of shapes of S_i and of values of κ and D is that the stored temperature fields can evolve into a discrete multidimensional temperature field that is sufficiently dense for interpolation between field values. It follows that a discrete multidimensional temperature field, having been constructed and sufficiently dense, can be used for objective function minimization as an alternative to parametric representation using basis functions. It follows that an alternative parameterization to that using the basis functions defined by Eq 8-12 is given by

$$T(\hat{x}, t, \kappa, V) = T_A + \sum_{i=1}^{N_i} A_i T(\hat{x}_i, t, \kappa, V_i, D, S_{it}, S_{il}, S_{its}) \quad \text{and}$$
$$T(\hat{x}_n^c, t_n^c, \kappa) = T_n^c \qquad \text{(Eq 14)}$$

where A_i, $i = 1,\ldots, N_i$, are weight coefficients for effecting interpolation within the multidimensional space defined by $(\hat{x}, t, \kappa, V, D, S_{it}, S_{il}, S_{its})$. As with the basis functions defined by Eq 6 and 7, which are based on a generalized function representation, the multidimensional functions $T(\hat{x}, t, \kappa, V, D, S_{it}, S_{il}, S_{its})$ provide for the specification of a numerical basis function representation of the temperature field.

The general procedure for constructing a multidimensional temperature field entails calculation of the time-dependent temperature field for a specified range of sizes and shapes of the inner surface boundary S_i for a given welding, or in general, heat deposition process. In the case of welding processes, rather than constructing a temperature field that is a function of a closed surface S_i, a more realistic construction should consider temperature field dependence on the experimentally observable solidification boundaries S_{it}, S_{il}, and S_{its} that are shown in Fig. 4. Construction of a multidimensional temperature field follows by adjustment of process parameters such that S_{it}, S_{il}, and S_{its} span a range of values that include all process conditions. For each set of values of S_{it}, S_{il}, and S_{its}, temperature histories $T(\hat{x}, t, \kappa, V, D, S_{it}, S_{il}, S_{its})$ are calculated for specified values of κ, V and D. This procedure is then followed for incremental changes of the parameters κ, V and D.

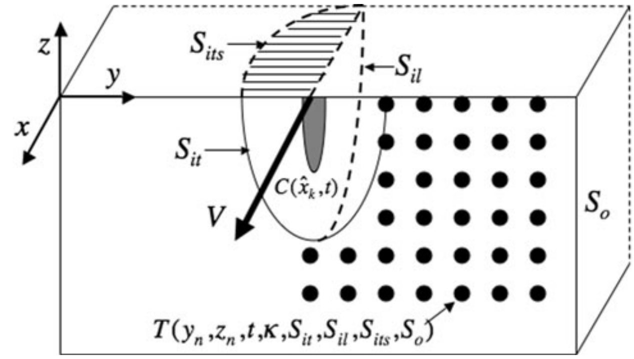

Fig. 4 Temperature field parameterization with respect to experimentally observable solidification boundaries

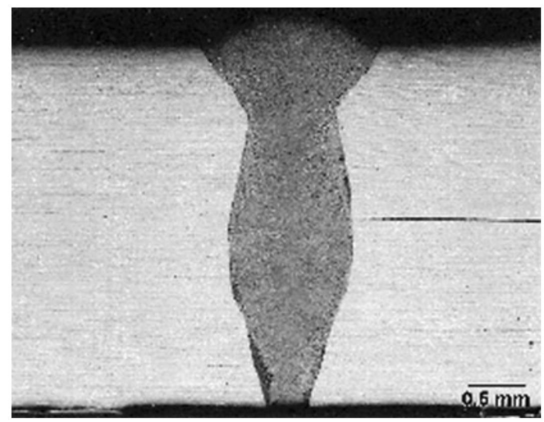

Fig. 5 Transverse cross section of deep-penetration weld adopted for prototype analysis

5. Prototype Analysis

In this section, a prototype analysis of a deep-penetration laser weld of 21-6-9 stainless steel is considered that was made using a Diode-Pumped Continuous Wave (CW) Nd:YAG laser at a welding speed of 45 ipm (1.905 cm/s) and helium as a shielding gas (see Fig. 5). The cross section of the workpiece is 0.12×0.68 in. (3.05×17.23 mm) and the top of the keyhole is located 0.28 and 0.4 in. from the two edges of the workpiece. The constraint conditions (y_c, z_c) on the transverse cross section of the solidification boundary are given in Table 1.

Considered first are calculations of the temperature field that adopt a temperature independent diffusivity $\kappa = 5 \times 10^{-6}$ $m^2\ s^{-1}$ and an adjusted discrete spatial distribution of the effective heat source given by Eq 7 so that the calculated cross sections of the solidification boundary satisfy the above constraint conditions given in Table 1. The results of these calculations are shown in Fig. 6(a) and 7 for the weighted sums of basis functions Eq 8; and in Fig. 6(b) and 8 for the weighted sums of basis functions Eq 11. The weighted sums of basis functions Eq 8 and 11 are shown schematically in Fig. 3(a) and (b), respectively. For the parameterization defined by Eq 8, the temperature field was calculated using the parameter values $\Delta t = 5.7 \times 10^{-3}$ s, $N_t = 80$, $t_k - t_{k-1} = 5\Delta t$, $x_k - x_{k-1} =$ 0.508 mm and $\{q(z_0),\ldots,q(z_{13})\}$ = {5.5, 1.8, 0.9, 0.75, 0.9, 1.3, 1.5, 1.4, 1.15, 0.9, 0.675, 0.48, 0.35}, where $z_k = 0.254k$ mm, $k = 0,\ldots, 13$. For the parameterization defined by Eq 11, the temperature field was calculated using the parameter values $\Delta t = 5.4 \times 10^{-3}$ s, $N_t = 80$, $V_k = 1.905$ cm/s and $\{q(z_0),\ldots, q(z_{13})\} = \{1.3, 0.8, 0.4, 0.4, 0.4, 0.6, 0.75, 0.7, 0.65, 0.6, 0.55, 0.35, 0.25\}$, where $z_k = 0.254k$ mm, $k = 0,\ldots, 13$.

Table 1 Temperature field constraint conditions at positions (y_c, z_c) on transverse cross section at solidification boundary

y_c, mm	z_c, mm
0.75	0.0
0.375	0.5
0.438	0.875
0.5	1.438
0.438	2.063
0.313	2.5
0.188	2.938

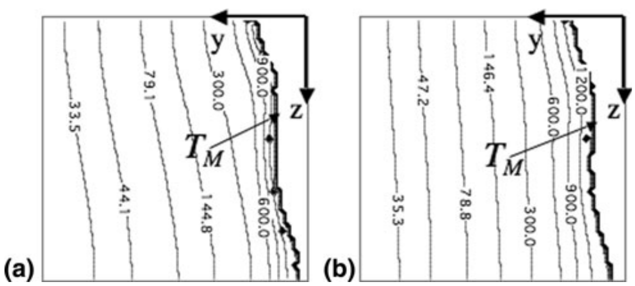

Fig. 6 Temperature field (°C) at transverse cross section of weld at time $t = 0.133$ s calculated according to transformation $x = Vt$, where $t = 0$ is at $x = 0$ in Fig. 7 and 8. (a) Temperature field calculated using basis functions defined by Eq 8 through 10; (b) temperature field calculated using basis functions defined by Eq 11 and 12

Considered next are temperature-field calculations demonstrating spatial modulation and filtering of the heat diffusion pattern according to adjustment of the various parameters associated with generalizations of the weighted sums of basis functions defined by Eq 8 through 12.

6. Spatially Modulated and Filtered Parameterizations Using Analytical Basis Functions

As demonstrated by the prototype analysis given above, the parametric representation defined by Eq 8 through 12 is sufficiently flexible for construction of temperature fields associated with heat deposition processes where source and workpiece characteristics are relatively simple. It is significant to note, however, that many energy deposition processes are characterized by volumetric coupling of the energy source and associated diffusion patterns that are relatively complex. Accordingly, it would be advantageous to extend the adjustability of the mapping defined by Eq 13 for the purpose of representing more complex diffusion patterns. The adjustability of the parameterization can be extended by adopting basis functions whose spatial distributions are spatially modulated and filtered. Among the many different possible types of spatial modulation and filtering that can be applied are those whose application produces diffusion patterns that are directionally or path weighted. The extension of the mapping defined by Eq 13 for the inclusion of spatial modulation and filtering is such that

$$T(\hat{x}, t, \kappa, V, D, T_s(\hat{x}_S), \hat{x}_S \in S_{\mathrm{i}}, S_{\mathrm{o}}) = W(\hat{x})T(\hat{x}, t, \kappa_m(\hat{x}), C(\hat{x}_k), \hat{x}_k, t_k, \Delta t, N_t, N_k, V_k), \quad \text{(Eq 15)}$$

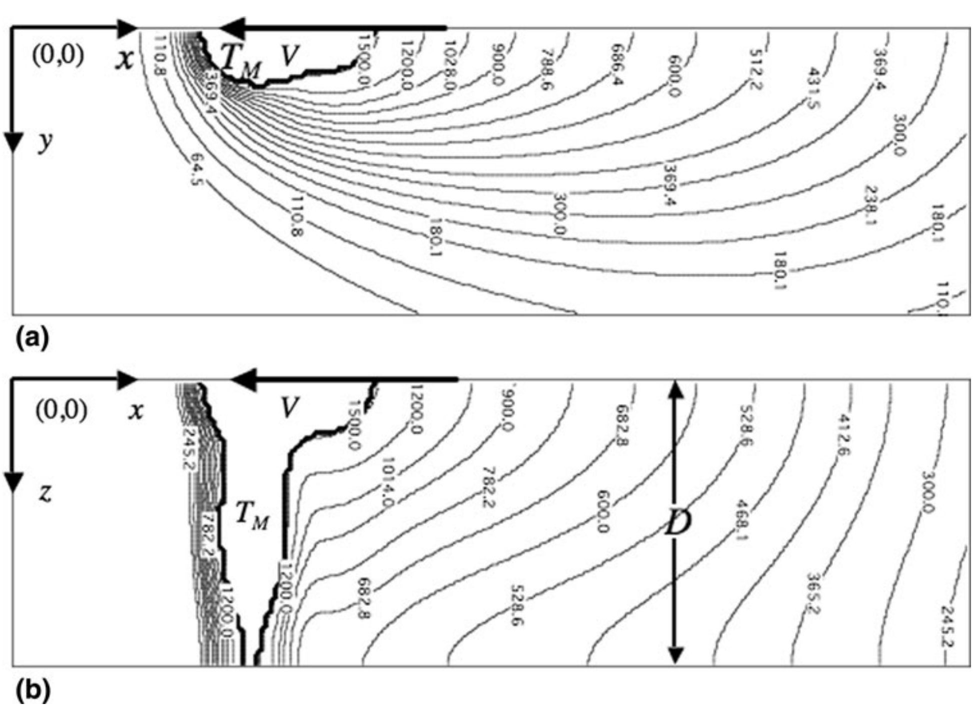

Fig. 7 Slices of three-dimensional temperature field (°C) calculated using basis functions defined by Eq 8 through 10, and solidification cross section shown in Fig. 5 as constraint condition. (a) Temperature field (°C) over top surface of workpiece; (b) temperature field (°C) over longitudinal slice at symmetry plane; where $D = 3.05$ mm

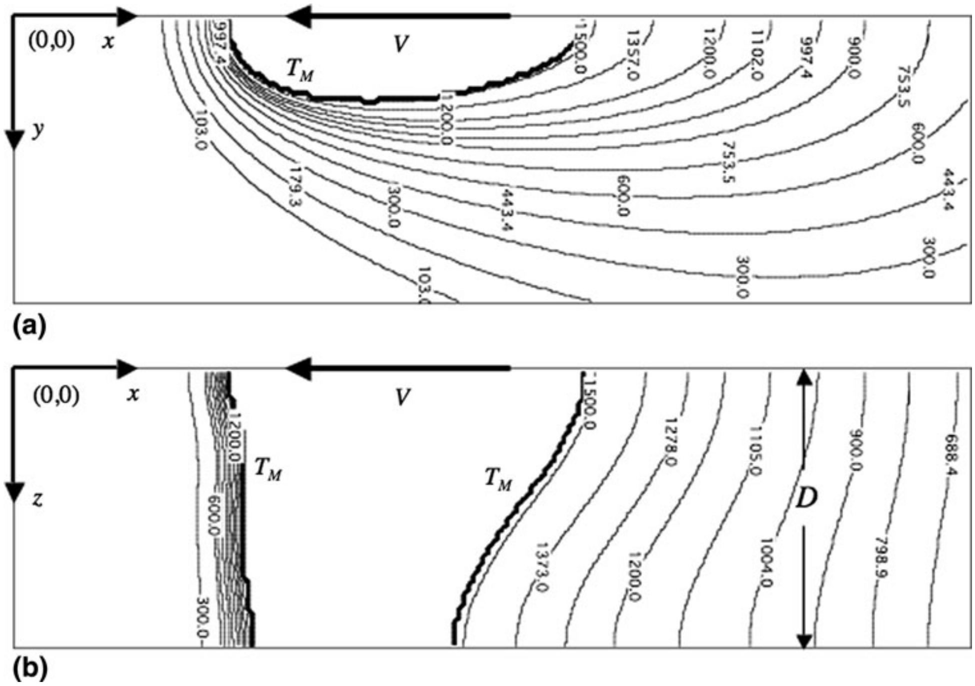

Fig. 8 Slices of three-dimensional temperature field (°C) calculated using basis functions defined by Eq 11 and 12, and solidification cross section shown in Fig. 5 as constraint condition. (a) Temperature field (°C) over top surface of workpiece; (b) temperature field (°C) over longitudinal slice at symmetry plane; where $D = 3.05$ mm

where $W(\hat{x})$ represents a spatial filter function and the associated weighted sums of basis functions are

$$T(\hat{x},t) = T_A + \sum_{k=1}^{N_k}\sum_{n=1}^{N_t} C(\hat{x}_k)F(\hat{x},\hat{x}_k,n\Delta t,\kappa_m(\hat{x}))\delta(n\Delta t - t_k) \quad \text{(Eq 16)}$$

where

$$F(\hat{x},\hat{x}_k,t,\kappa_m(\hat{x})) = \frac{1}{t}\exp\left[-\frac{(x-x_k)^2+(y-y_k)^2}{4\kappa_m(\hat{x})t}\right] \times \left\{1+2\sum_{m=1}^{\infty}\exp\left[-\frac{\kappa_m(\hat{x})m^2\pi^2 t}{l^2}\right]\cos\left[\frac{m\pi z}{l}\right]\cos\left[\frac{m\pi z_k}{l}\right]\right\} \times (\cos\theta)^{2p} \quad \text{(Eq 17)}$$

and

$$T(\hat{x},t) = T_A + \sum_{k=1}^{N_k}\sum_{n=1}^{N_t} C(\hat{x}_k)G(\hat{x},\hat{x}_k,n\Delta t,V_k,\kappa_m(\hat{x})) \quad \text{(Eq 18)}$$

where

$$G(\hat{x},\hat{x}_k,t,V_k,\kappa_m(\hat{x})) = \frac{1}{t}\exp\left[-\frac{(x-x_k-V_k t)^2+(y-y_k)^2}{4\kappa_m(\hat{x})t}\right] \times \left\{1+2\sum_{m=1}^{\infty}\exp\left[-\frac{\kappa_m(\hat{x})m^2\pi^2 t}{l^2}\right]\cos\left[\frac{m\pi z}{l}\right]\cos\left[\frac{m\pi z_k}{l}\right]\right\} \times (\cos\theta)^{2p} \quad \text{(Eq 19)}$$

Referring to Eq 16 through 19, it is to be noted that spatial modulation and filtering of the diffusion field is through functional dependence, respectively, on the factor $(\cos\theta)^{2p}$, where integer $p \geq 1$, the generalized diffusivity function $\kappa_m(\hat{x})$ and the adjustable parameters $\Delta t, N_t, N_k$ and V_k. In its simplest form $\kappa_m(\hat{x}) = \kappa_o$, a constant value not equal to the average diffusivity κ of the material of the workpiece. Accordingly, $\kappa_m(\hat{x})$ can be generalized to represent a spatially weighted average of diffusivities such as

$$\kappa_m(x) = (1 - x/L)\kappa_1 + (x/L)\kappa_2 \quad \text{(Eq 20)}$$

or a path dependent diffusivity function, which in general is given by

$$\kappa_m(r,\theta) = \frac{1}{r}\int_0^r \kappa(r',\theta)dr' = \frac{1}{r}\sum_{k=1}^{N_k}\kappa(k\Delta r,\theta)\Delta r = \frac{1}{N_k}\sum_{k=1}^{N_k}\kappa(k\Delta r,\theta), \quad \text{(Eq 21)}$$

given that a function $\kappa_m(\hat{x})$ has been specified. Similarly, the parameter V_k, which can be a function of the discrete index k, can assume values that are in general not equal to the speed of the energy source V relative to the workpiece.

At this point it should be instructive to consider temperature field calculations demonstrating spatial modulation and filtering of the heat diffusion pattern according to adjustment of the various parameters associated with the weighted sums of basis functions defined by Eq 16 through 19. The results of these calculations are shown in Fig. 9 through 11. The purpose of these calculations is only to demonstrate some general functional characteristics associated with the adjustment of the generalized parameterization defined by Eq 16 through 19. Shown in Fig. 9 is a two-dimensional slice of a three-dimensional temperature field that was calculated using the basis functions defined by Eq 18 and 19 with the parameter values $\kappa = 5 \times 10^{-6}$ m^2 s^{-1}, $\Delta t = 5.4 \times 10^{-3}$ s, $N_t = 80$,

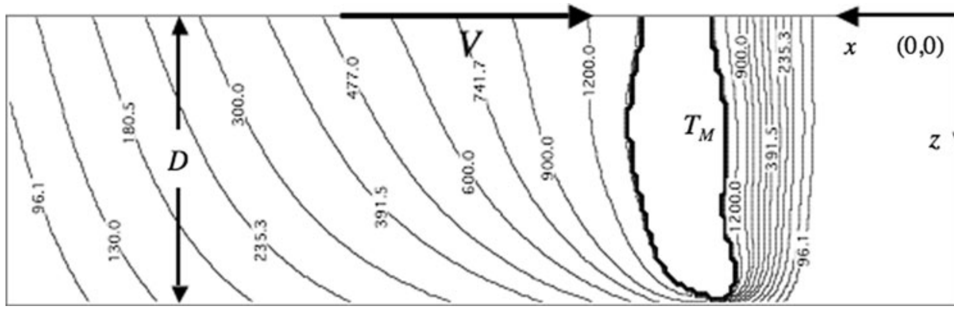

Fig. 9 Slice of three-dimensional temperature field (°C) at symmetry plane calculated using basis functions defined by Eq 18 and 19 with $p = 3$, where $D = 3.05$ mm

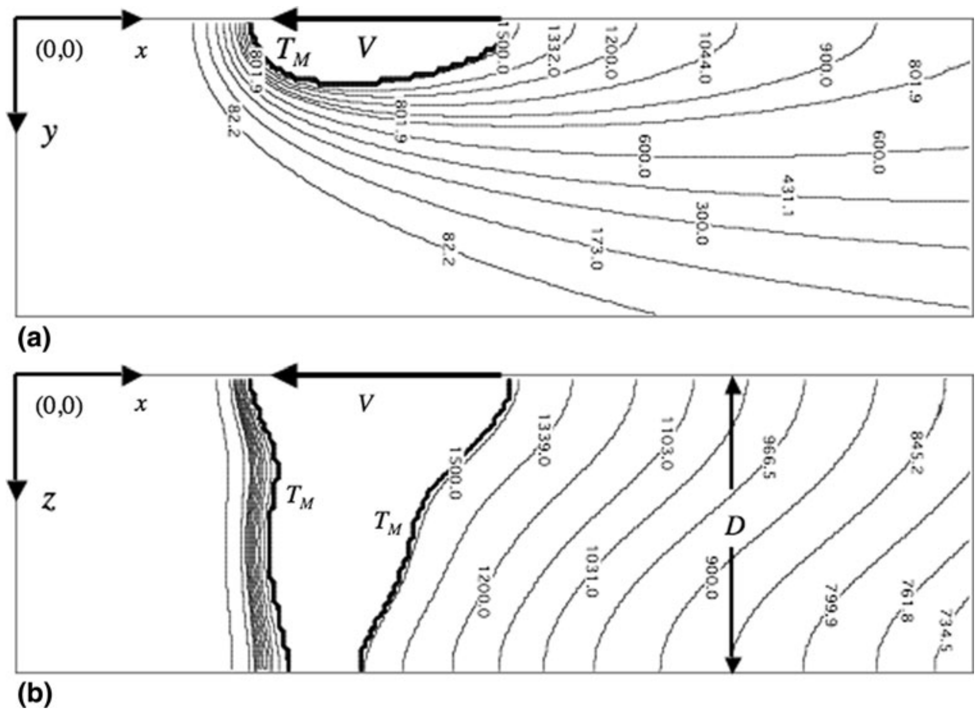

Fig. 10 Slices of three-dimensional temperature field (°C) calculated using basis functions defined by Eq 11 and 12 with parameter V_k assumed adjustable. (a) Temperature field (°C) over top surface of workpiece; (b) temperature field (°C) over longitudinal slice at symmetry plane; where $D = 3.05$ mm

$V_k = 1.5$ cm/s, $p = 3$ and $\{q(z_0),\ldots, q(z_{13})\} = 0.65 \times \{1.3, 0.8, 0.4, 0.4, 0.4, 0.6, 0.75, 0.7, 0.65, 0.6, 0.55, 0.35, 0.25\}$, where $z_k = 0.254k$ mm, $k = 0,\ldots, 13$. Similarly, shown in Fig. 10 is a two-dimensional slice of a three-dimensional temperature field that was calculated using the parameter values $\kappa = 5 \times 10^{-6}$ m^2 s^{-1}, $\Delta t = 5.4 \times 10^{-3}$ s, $N_t = 80$, $V_k = 3.0$ cm/s, and $\{q(z_0),\ldots,q(z_{13})\} = \{1.3, 0.8, 0.4, 0.4, 0.4, 0.6, 0.75, 0.7, 0.65, 0.6, 0.55, 0.35, 0.25\}$, where $z_k = 0.254k$ mm, $k = 0,\ldots, 13$. And finally, shown in Fig. 11 is a two-dimensional slice of a three-dimensional temperature field that was calculated using the parameter values $\kappa = 4 \times 10^{-6}$ m^2 s^{-1}, $\Delta t = 5.4 \times 10^{-3}$ s, $N_t = 40$, $V_k = 3.0$ cm/s, and $\{q(z_0),\ldots,q(z_{13})\} = \{1.3, 0.8, 0.4, 0.4, 0.4, 0.6, 0.75, 0.7, 0.65, 0.6, 0.55, 0.35, 0.25\}$, where $z_k = 0.254k$ mm, $k = 0,\ldots, 13$.

The necessity of a more general and flexible parameterization follows from the specific definition of the inverse heat transfer problem that is considered here, and the associated conditions for its application. That is, the goal of any inverse analysis following the general procedure considered here is construction of a temperature field $T(\hat{x}, t, \kappa, V, D, T_s(\hat{x}_S), \hat{x}_S \in S_\mathrm{i}, S_\mathrm{o})$ where the surface distribution of temperatures $T_s(\hat{x}_S), \hat{x}_S \in S_\mathrm{i}, S_\mathrm{o}$, represents the only constraint condition on the calculated temperature field. Accordingly, parameterizations that are sufficiently flexible and convenient with respect to variation of heat diffusion patterns are required.

7. Parameterizations Using Self-Similarity Transformations

The definition of inverse heat transfer problem presented above provides a foundation for the application of relatively more general parameterizations of heat deposition processes for their inverse analysis. Presented in this section

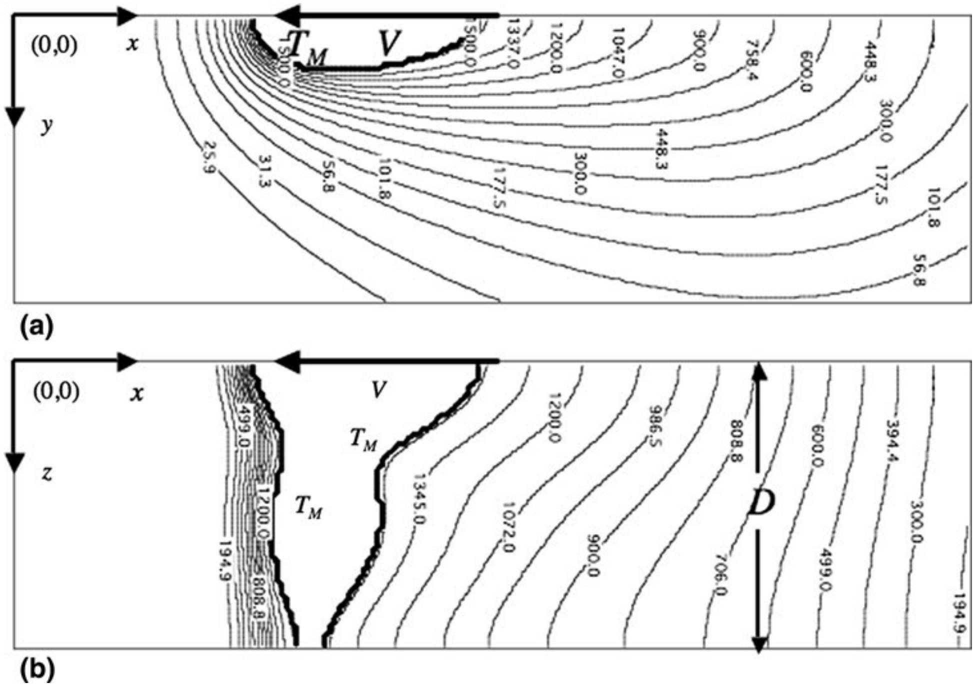

Fig. 11 Slices of three-dimensional temperature field (°C) calculated using basis functions defined by Eq 11 and 12 with parameters κ and V_k assumed adjustable. (a) Temperature field (°C) over top surface of workpiece; (b) temperature field (°C) over longitudinal slice at symmetry plane; where $D = 3.05$ mm

is a preliminarily proof showing that, in addition to providing for more general parameterizations, the definition of the inverse heat transfer problem considered here provides a foundation for the application of similarity transformations to such analyses. A consequence of the practical application of similarity transformations to inverse analysis of heat deposition is that flexible and convenient parameterizations are required.

Proceeding and assuming that the diffusivity function $\kappa(\hat{x}, t)$ is not characterized by large spatial or temporal variation, Eq 1a can assume the form

$$\frac{\partial T(\hat{x}, t)}{\partial t} = \kappa(\hat{x}, t)\nabla^2 T(\hat{x}, t) \qquad \text{(Eq 22)}$$

Next, by applying a change of variables according to the relation $x = Vt$, it follows that

$$V\frac{\partial T(\hat{x})}{\partial x} = \kappa(\hat{x})\nabla^2 T(\hat{x}) \qquad \text{(Eq 23)}$$

Next, Eq 23 is reformulated in terms of a discrete finite-difference representation, i.e.,

$$V\left(\frac{T_p - T_{p-1}}{\Delta l}\right) = \frac{\kappa_p}{(\Delta l)^2}\left(\sum_{n=1}^{6} T_n - 6T_p\right) \qquad \text{(Eq 24)}$$

where V is the speed of energy deposition relative to the workpiece, Δl is the distance between discrete positions representing a discrete partitioning of the volume of the workpiece, and the discrete indices p, $p-1$ and n are defined in Fig. 12. It follows from Eq 24 that the discrete diffusivity field κ_p as a function of discrete grid-location p is given by

$$\kappa_p = V\Delta l(T_p - T_{p-1})\left(\sum_{n=1}^{6} T_n - 6T_p\right)^{-1}. \qquad \text{(Eq 25)}$$

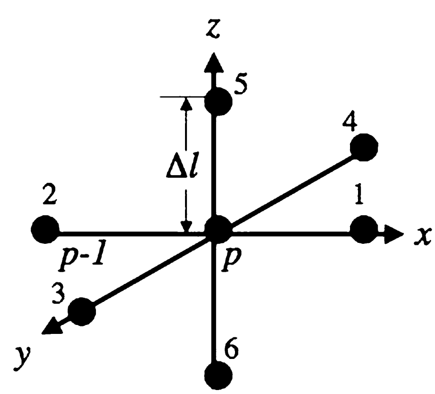

Fig. 12 Indexing scheme for discrete finite-difference representation of heat conduction equation given by Eq 24

7.1 Discussion

Referring to Eq 25, one notes that this expression implies a similarity transformation where a discrete three-dimensional temperature field, whose values T_p are a function of discrete index p, can be mapped onto a family of discrete diffusivity fields κ_p by means of the linear scaling parameters V and Δl. It follows then that the generalized parameterizations presented above can be adopted for construction of a discrete temperature field T_p that is defined by a specific diffusion pattern, but is yet independent of space and time scales. This discrete temperature field can then be scaled spatially and temporal by adjusting the parameters V and Δl according to the specified speed of energy deposition and distribution of temperatures $T_s(\hat{x}_S)$ (where $\hat{x}_S \in S_{\mathrm{i}}, S_{\mathrm{o}}$), respectively. Again referring to Eq 25, and consistent with the inverse analysis approach, the material property

κ_p is a quantity that can be deduced rather than adopted as input information for the model system. Given the similarity transformation defined by Eq 25, it follows that the temperature fields whose cross sections are shown in Fig. 7 through 11 can be arbitrarily adjusted parametrically and then rescaled spatially and temporally in order to satisfy different types of process conditions.

8. Conclusion

The objective of this report was to present a preliminary description of general and flexible parameterizations of time-dependent temperature fields occurring in heat deposition processes that include spatial modulation and filtering of diffusion patterns. These generalized parameterizations follow from a specific and restricted definition of the inverse heat transfer problem. The specific algorithmic aspects of constructing temperature fields by means of these parameterizations are for further investigation. The specific definition of the inverse heat transfer problem presented here provides a foundation for application of similarity transformation to inverse analysis of heat deposition processes. Accordingly, generalized and flexible parameterizations are significant for the application of similarity transformations to the inverse analysis of such processes. That is, the application of similarity transformations requires the ability to construct three-dimensional temperature fields characterized by heat diffusion patterns having a wide range of variation in their spatial distribution. Further examination of the parameterizations presented here and of the application of similarity transformations is more appropriate within the context of inverse analysis applied to specific systems.

Acknowledgment

One of the authors (SGL) acknowledges the support by the Naval Research Laboratory (NRL) internal core program.

References

1. D.N. Ghosh Roy, *Methods of Inverse Problems in Physics*, CRC Press, Boca Raton, 1991
2. K.A. Woodbury, Ed., *Inverse Engineering Handbook*, CRC Press, New York, 2003
3. A. Tarantola, *Inverse Problem Theory and Methods for Model Parameter Estimation*, SIAM, Philadelphia, PA, 2005
4. C.R. Vogel, *Computational Methods for Inverse Problems*, SIAM, Philadelphia, PA, 2002
5. P.C. Sabatier, Ed., *Inverse Problems: An Interdisciplinary Study*, Academic Press, London, 1987
6. C.W. Groetsch, *Inverse Problems in the Mathematical Sciences*, Vieweg, Bruanschweig, Wiesbaden, 1993
7. A. Kirsch, *An Introduction to the Mathematical Theory of Inverse Problems*, Springer-Verlag, New York, 1996
8. A.G. Ramm, *Inverse Problems, Mathematical and Analytical Techniques with Applications to Engineering*, Springer Science, New York, 2005, p 9–10
9. I.J.D. Craig and J.C. Brown, *Inverse Problems in Astronomy, A Guide to Inversion Strategies for Remotely Sensed Data*, Adam Hilger Ltd, Bristol and Boston, 1986
10. M.N. Ozisik and H.R.B. Orlande, *Inverse Heat Transfer, Fundamentals and Applications*, Taylor and Francis, New York, 2000
11. K. Kurpisz and A.J. Nowak, *Inverse Thermal Problems*, Computational Mechanics Publications, Boston, 1995
12. O.M. Alifanov, *Inverse Heat Transfer Problems*, Springer, Berlin, 1994
13. J.V. Beck, B. Blackwell, and C.R. St. Clair, *Inverse Heat Conduction: Ill-Posed Problems*, Wiley Interscience, New York, 1985
14. J.V. Beck, Inverse Problems in Heat Transfer with Application to Solidification and Welding, *Modeling of Casting, Welding and Advanced Solidification Processes*, V.M. Rappaz, M.R. Ozgu, and K.W. Mahin, Ed., The Minerals, Metals and Materials Society, Warrendale, 1991, p 427–437
15. J.V. Beck, Inverse Problems in Heat Transfer, *Mathematics of Heat Transfer*, G.E. Tupholme and A.S. Wood, Ed., Clarendon Press, Oxford, 1998, p 13–24
16. N. Zabaras, Inverse Modeling of Solidification and Welding Processes, *Modeling of Casting, Welding and Advanced Solidification Processes*, V.M. Rappaz, M.R. Ozgu, and K.W. Mahin, Ed., The Minerals, Metals and Materials Society, Warrendale, 1991, p 523–530
17. G.S. Dulikravich and T.J. Martin, Inverse Shape and Boundary Condition Problems and Optimization, *Heat Conduction: Advances in Numerical Heat Transfer*, Vol 1, Chap. 10, W.J. Minkowycz and E.M. Sparrow, Ed., Taylor & Francis, London, 1996, p 381–426
18. T.J. Martin and G.S. Dulikravich, Inverse Determination of Boundary Conditions in Steady Heat Conduction with Heat Generation, *ASME J. Heat Transfer*, 1996, **118**, p 546–554
19. J. Xie and J. Zou, Numerical Reconstruction of Heat Fluxes, *SIAM J. Numer. Anal.*, 2005, **43**(4), p 1504–1535
20. S.G. Lambrakos and J.G. Michopoulos, Algorithms for Inverse Analysis of Heat Deposition Processes, *Mathematical Modelling of Weld Phenomena*, Vol 8, Verlag der Technischen Universite Graz, Austria, 2007, p 847
21. S.G. Lambrakos and J.G. Michopoulos, Computational Parameterization Simplicity and Filtering of Data-Driven Inverse Analysis for Heat Deposition Processes, *Proceedings of IDETC/CIE 2006, ASME 2006 International Design Engineering Technical Conferences & Computers and Information in Engineering Conference*, Sept 10–13, 2006, Philadelphia, PA
22. S.G. Lambrakos and J.O. Milewski, Analysis of Welding and Heat Deposition Processes Using an Inverse-Problem Approach, *Mathematical Modelling of Weld Phenomena*, Vol 7, Verlag der Technischen Universite Graz, Austria, 2005, p 1025–1055
23. P.G. Moore, H.N. Jones III, and S.G. Lambrakos, An inverse Heat Transfer Model of Thermal Degradation Within Multifunctional Tensioned Cable Structures, *J. Mater. Eng. Perform.*, **14**(1), Feb 2005
24. S.G. Lambrakos and J.O. Milewski, Analysis of Processes Involving Heat Deposition Using Constrained Optimization, *Sci. Technol. Weld. Join.*, 2002, **7**(3), p 137
25. S.G. Lambrakos and D.W. Moon, Analysis of Welds Using Geometric Constraints, *Computer-Aided Design, Engineering, and Manufacturing, Systems Techniques and Applications*, C. Leondes, Ed., CRC Press, New York, 2001
26. S.G. Lambrakos, E.A. Metzbower, J.O. Milewski, G. Lewis, R. Dixon, and D. Korzekwa, Simulation of Deep Penetration Welding Processes Using Geometric Constraints Based on Experimental Information, *J. Mater. Eng. Perform.*, 1994, **3**(5), p 639
27. K.P. Cooper and S.G. Lambrakos, Fabrication of Net-Shaped Metallic Parts by Overlapping Reinforcement Weld Beads, *Proceedings of the Seventh International Conference on Trends in Welding Research*, May 16–20 (Pine Mountain, GA), ASM International, Materials Park, OH, 2005, p 647
28. E.A. Metzbower, D.W. Moon, C.R. Feng, S.G. Lambrakos, and R.J. Wong, Modelling of HSLA-65 GMAW Welds, *Mathematical Modelling of Weld Phenomena*, Vol 7, Verlag der Technischen Universite Graz, Austria, 2005, p 327–339
29. S.G. Lambrakos, R.W. Fonda, J.O. Milewski, and J.E. Mitchell, Analysis of Friction Stir Welds Using Thermocouple Measurements, *Sci. Technol. Weld. Join.*, 2003, **8**, p 345
30. R.W. Fonda and S.G. Lambrakos, Analysis of Friction Stir Welds Using an Inverse Problem Approach, *Sci. Technol. Weld. Join.*, 2002, **7**(3), p 177
31. J. Hadamard, 'Sur les problèmes aux dérivées partielles et leur signification physique', Princeton University Bulletin, 1902, p 49-52
32. *Proceedings International Conferences on Trends in Welding Research*, Vol 1–7, ASM International, Materials Park, OH

33. *Mathematical Modelling of Weld Phenomena*, Vol 1–8, Verlag der Technischen Universite Graz, Austria
34. J.A. Goldak and M. Akhlaghi, *Computational Welding Mechanics*, Springer Science+Business Media, Inc., 2005
35. J. Goldak, A. Chakravarti, and M. Bibby, A New Finite Element Model for Welding Heat Source, *Metall. Trans. B*, 1984, **15**, p 299–305
36. J. Goldak, M. Bibby, J. Moore, R. House, and B. Patel, Computer Modeling of Heat Flow in Welds, *Metall. Trans. B*, 1986, **17**, p 587–600
37. R.N. Bracewell, *The Fourier Transform and Its Applications*, 2nd ed., McGraw-Hill Book Company, New York, 1986, p 345–355
38. V.A. Karkhin, V.V. Plochikhine, A.S. Ilyin, and H.W. Bergmann, Inverse Modelling of Fusion Welding Process, *Mathematical Modelling of Weld Phenomena 6*, H. Cerjak, Ed., Maney Publishing, London, 2002, p 1017–1042
39. V.A. Karkhin, V.V. Plochikhine, and H.W. Bergmann, Solution of Inverse Heat Conduction Problem for Determining Heat Input, Weld Shape, and Grain Structure During Laser Welding, *Sci. Technol. Weld. Join*., 2002, **7**(4), p 224–231
40. V.A. Karkhin, P.N. Homich, and V.G. Michailov, Models for Volume Heat Sources and Functional-Analytic Technique for Calculating the Temperature Fields in Butt Welding, *Mathematical Modelling of Weld Phenomena*, Vol 8, Verlag der Technischen Universite Graz, Austria, 2007, p 847
41. V.A. Karkhin, V.G. Michailov, and V.D. Akatsevich, Modelling the Thermal Behaviour of Weld and Heat-Affected Zone During Pulsed Power Welding, *Mathematical Modelling of Weld Phenomena 4*, H. Cerjak, Ed., The University Press, Cambridge, 1998, p 411–426
42. S. Kou, *Welding Metallurgy*, 2nd ed., Wiley-Interscience, New York, 2002
43. E.A. Metzbower, Laser Beam Welding: Thermal Profiles and HAZ Hardness, *Weld. J.*, 1990, **69**(7), p 272
44. I. Tosello, F.X. Tissot, and M. Barras, Modelling of Weld Behaviour for the Control of the GTA Process by Computer Aided Welding, *Mathematical Modelling of Weld Phenomena 4*, H. Cerjak and H.K.D.H. Bhadeshia, Ed., IOM Communications Ltd, London, 1998, p 80–103
45. R.C. Reed and H.K.D.H. Bhadeshia, A Simple Model for Multipass Welds, *Acta Metall. Mater.*, 1994, **42**(11), p 3663–3678
46. M. Maalekian, E. Kozeschnik, H.P. Brantner, and H. Cerjak, Inverse Modelling of Heat Generation in Friction Welding, *Mathematical Modelling of Weld Phenomena*, Vol 8, Verlag der Technischen Universite Graz, Austria, 2007, p 881–890
47. N.N. Rykalin, *Thermal Fundamentals of Welding*, USSR Academy of Sciences, Moscow-Leningrad, 1947
48. N.N. Rykalin, *Calculation of Heat Flow in Welding*, Z. Paley and C.M. Adams, Trans., 1951
49. N.N. Rykalin, *Berchnung der Wdrmevorgange beim Schweissen*, VEB, Ed., Verlag Technik, Berlin, 1957
50. N.N. Rykalin, Energy Sources for Welding, *Weld. World*, 1974, **12**(9/10), p 227–248
51. P.N. Sabapathy, M.A. Wahab, and M.J. Painter, Numerical Methods to Predict Failure During the In-Service Welding of Gas Pipelines, *J. Strain Anal.*, 2001, **36**(6), p 611–619
52. E. Ranatowski and A. Pocwiardowski, An Analytical-Numerical Evaluation of the Thermal Cycle in the HAZ During Welding, *Mathematical Modelling of Weld Phenomena 4*, H. Cerjak and H.K.D.H. Bhadeshia, Ed., IOM Communications Ltd, London, 1998, p 379–395
53. E. Ranatowski and A. Pocwiardowski, An Analytical-Numerical Estimation of the Thermal Cycle During Welding with Various Heat Source Models Application, *Mathematical Modelling of Weld Phenomena 5*, H. Cerjak and H.K.D.H. Bhadeshia, Ed., IOM Communications Ltd, London, 1998, p 723–742
54. E. Ranatowski and A. Pocwiardowski, An Analytical-Numerical Assessment of the Thermal Cycle in HAZ with Three Dimensional Heat Source Models and Pulsed Power Welding, *Mathematical Modelling of Weld Phenomena 7*, H. Cerjak, H.K.D.H. Bhadeshia, and E. Kozeschnik, Ed., Verlag der Technischen Universite Graz, Austria, 2001, p 1111–1128
55. D. Rosenthal, The Theory of Moving Sources of Heat and Its Application to Metal Treatments, *Trans. ASME*, 1946, **68**, p 849–866
56. D. Rosenthal, *Weld. J.*, 1941, **20**, p 220s–241s
57. D. Rosenthal, Etude theoretic du regime thermique pendant la soudure a l'arc, 2ieme Congress National des Sciences, Brussels, 1935, p 1277–1292
58. O. Grong, *Metallurgical Modelling of Welding*, 2nd ed., Chap 2, Materials Modelling Series, H.K.D.H. Bhadeshia, Ed., The Institute of Materials, UK, 1997, p 1–115
59. H.S. Carslaw and J.C. Jaegar, *Conduction of Heat in Solids*, 2nd ed., Clarendon Press, Oxford, 1959, p 374